ARTICLE

Movements and oceanographic associations of bigeye tuna (*Thunnus obesus*) in the Northwest Atlantic

Chi Hin Lam, Benjamin Galuardi, and Molly E. Lutcavage

Abstract: To address the lack of fisheries-independent information for Atlantic bigeye tuna (*Thunnus obesus*), we released 21 adults (131 ± 12 cm curved fork length) between 2008 and 2010 in the Sargasso Sea and Northwest Atlantic. Data from nine tags (range: 1–292 days; mean: 89 days) revealed (*i*) pronounced north–south movements in pelagic waters between areas including Georges Bank, Mid- and South Atlantic Bight, Caribbean Sea, and Brazilian shelf, (*ii*) a lack of east–west exchange, and (*iii*) a high-use area in the Hatteras Plain, centered southwest of Bermuda. Bigeye tuna occupied water masses of 2.7–28.2 °C and depths of 0–1280 m, with deeper depths in the daytime (daily mean ± standard deviation: 196 ± 92 m) than at nighttime (45 ± 29 m). Even though bigeye tuna are assumed to forage on the deep scattered layer during the day, generalized additive mixed models did not identify the deep scattered layer as an important predictor of daytime swimming depth. Model results highlight the importance of geographic location in influencing habitat utilization, and thus suggest the need for fisheries-independent monitoring in high-catch areas, such as the central and equatorial Atlantic.

Résumé : Pour pallier l'absence d'information indépendante des pêches concernant le thon obèse (*Thunnus obesus*) de l'Atlantique, nous avons relâché 21 adultes (131 ± 12 cm longueur à la fourche incurvée) de 2008 à 2010, dans la mer des Sargasses et le nord-ouest de l'Atlantique. Des données de neuf étiquettes (intervalle : 1–292 jours; moyenne: 89 jours) ont révélé (*i*) des déplacements nord–sud marqués dans les eaux pélagiques entre différentes régions dont le banc de Georges, les golfes médio- et sud-atlantiques, la mer des Caraïbes et le plateau brésilien, (*ii*) l'absence d'échanges est–ouest et (*iii*) une région de forte utilisation dans la plaine abyssale d'Hatteras, centrée au sud-ouest des Bermudes. Les thons obèses occupaient des masses d'eau de 2,7 °C à 28,2 °C et des profondeurs de 0 m à 1 280 m, préférant de plus grandes profondeurs le jour (moyenne quotidienne ± SD: 196 ± 92 m) que la nuit (45 ± 29 m). Même s'il est présumé que les thons obèses se nourrissent dans la couche diffusante profonde le jour, des modèles mixtes additifs généralisés n'ont pas établi que la couche diffusante profonde était une importante variable prédictive de la profondeur de nage diurne. Les résultats des modèles mettent en évidence l'importante influence de l'emplacement géographique sur l'utilisation de l'habitat, soulignant ainsi la nécessité d'une surveillance indépendante des pêches dans les régions de forte capture comme l'Atlantique central et équatorial. [Traduit par la Rédaction]

Introduction

Bigeye tuna (*Thunnus obesus*) is one of the most important commercial tuna species in the Atlantic. It is most commonly found in tropical and subtropical waters, but is fished from 50°N to 50°S (Pallarés et al. 1996). The Atlantic population is managed as a single stock (Anonymous 2005, 2011*b*), based on genetics (Durand et al. 2005; Gonzalez et al. 2008; Martínez et al. 2006), spatiotemporal distribution of catch (Anonymous 2011*a*), and movements from conventional tagging (International Commission for the Conservation of Atlantic Tunas 2006; Zavala-Camin 1977). Tagging information, however, is particularly limited for the Northwest Atlantic. The International Commission for the Conservation of Atlantic Tunas (ICCAT) conventional tag database contains 11 198 conventional tags deployed but only 12 complete tag–recapture records originating from or terminated in this region between 1969 and 2009. To date, only two studies have utilized electronic tags to track Atlantic bigeye tuna (Arrizabalaga et al. 2008; Matsumoto et al. 2005). Tagging durations from these studies were relatively short (max. 113 days) and did not allow for seasonal analysis of movement or exploration of alternate stock composition hypotheses. Longer term movement information is needed to evaluate life history, habitat utilization, and alternative stock

scenarios (ICCAT 2006), such as northern and southern stocks (Anonymous 2005).

Much of the current knowledge on Atlantic bigeye tuna focuses on providing fisheries indices in support of stock assessment (Anonymous 2011*b*). Some biological parameters such as age and growth (summarized in Duarte-Neto et al. 2012), spawning time (Matsumoto and Miyabe 2002), and sexual maturity (Matsumoto and Miyabe 2002; Zhu et al. 2011) are established, mostly based on samples from the East or Central Atlantic. Minimum size for sexual maturity is estimated at 100–110 cm fork length. Drawing upon various studies on larval observations and maturity stage of gonads, Cayré et al. (1991) identified these common observations: (*i*) spawning occurs over a large geographical area around the Equator, spanning 15°N to 15°S in warm waters extending from the Gulf of Guinea to the American coasts; (*ii*) larvae occur in waters mostly above 24 °C (Rudomiotkina 1983) and up to 30 °C (Caverivière et al. 1976); and (*iii*) spawning occurs year-round, with the highest observed activity around the Gulf of Guinea from December to April, south of Brazil (0°S–10°S, 25°W–40°W) from January to June, and the Central North Atlantic between the northeastern coast of Brazil and the Gulf of Guinea (5°N–27°N, 25°W–60°W) from June to August. Movement and spatiotemporal distribution of bigeye tuna should reflect strategies of energy

C.H. Lam, B. Galuardi, and M.E. Lutcavage. Large Pelagics Research Center, University of Massachusetts, Amherst, 932 Washington Street, Gloucester, MA 01930, USA.

Corresponding author: Chi Hin Lam (e-mail: tagtuna@gmail.com).

Table 1. Tagging summary for adult bigeye tuna.

Tag ID	Mission (months)	CFL (cm)	Start date	End date	At liberty (days)	Data-days	Tag lat. (°N)	Tag long. (°W)	Report lat. (°N)	Report long. (°W)
2008-12722	12	127[a]	8 Dec. 2008				27.07	68.38		
2008-12863	12	111[a]	8 Dec. 2008				27.05	68.57		
2008-12865	12	124[a]	1 Dec. 2008				27.24	67.78		
2008-12975	12	136[a]	28 Nov. 2008	7 Jan. 2009	40	36	27.33	68.27	25.03	66.84
2009-12728	12	124[a]	5 Apr. 2009				30.70	75.36		
2009-12861	12	122[a]	23 Feb. 2009				28.32	68.97		
2009-12866	12	117[a]	4 Mar. 2009				26.37	70.23		
2010-14524	8	119[a]	28 Jan. 2010	1 June 2010	124	114	27.90	70.64	35.88	62.43
2010-14526	8	122[a]	27 Jan. 2010	14 May 2010	107	103	27.72	70.40	28.94	70.44
2010-14528	8	132	27 Nov. 2010				28.04	66.73		
2010-14535	8	144	24 Nov. 2010	22 Feb. 2011	90	86	28.49	67.08	5.80	40.81
2010-14537	8	135	23 Nov. 2010	29 Nov. 2010	6	1	28.48	67.22	28.48	67.57
2010-14707	8	119[a]	28 Jan. 2010				27.77	70.77		
2010-14709[b]	8	119[a]	27 Jan. 2010	12 Aug. 2011	562[b]	19	27.78	70.41	29.05	77.10
2010-14927	8	149	27 Nov. 2010				28.44	67.04		
2010-17271[b]	12	148	24 Oct. 2010	12 Aug. 2011	292[b]	292	39.78	70.62	40.29	68.14
2010-17272	12	133	28 Oct. 2010	15 Nov. 2010	18	14	39.72	71.28	34.35	68.43
2010-17276	12	148	27 Oct. 2010	14 Mar. 2011	138	134	39.77	71.26	38.08	66.60
2010-17279	12	150	1 Dec. 2010				28.59	68.37		
2010-17281	12	138	29 Oct. 2010				39.76	71.14		
2011-17329	12	134	17 June 2011				40.26	67.97		

Note: CFL, curved fork length.
[a]Estimated from length–weight relationship as specified in Parks et al. (1982).
[b]Recovered physically.

allocation and resource utilization, as demonstrated in bluefin tuna (Chapman et al. 2011).

Vertical movement of bigeye tuna is modulated by physiological constraints (Brill et al. 2005) and food availability (Bertrand et al. 2002). The diel swimming pattern with deeper daytime depths between 300 and 500 m is attributed to feeding on organisms associated with the deep (also called, sound) scattering layer (Josse et al. 1998; Dagorn et al. 2000; Matsumoto et al. 2013a), while oscillatory dives between deeper daytime depths and the surface mixed layer are hypothesized as being thermoregulatory behavior (Brill 1994; Holland et al. 1992; Schaefer and Fuller 2002; Musyl et al. 2003). Vertical movement data from archival tags are used in providing more reliable estimates of relative abundance (Bigelow et al. 2002), investigating fisheries management measures (Sibert et al. 2012) and climate change impacts (Lehodey et al. 2010) on tuna populations. However, in the Atlantic, short tag deployments (Matsumoto et al. 2005; Arrizabalaga et al. 2008) have so far returned only sparse records. To address this data gap, we applied methods for achieving long-term tag retention in bluefin tuna (Galuardi et al. 2010; Galuardi and Lutcavage 2012) and conducted the first pop-up satellite archival tag (PSAT) study on bigeye tuna in the Northwest Atlantic. We analyzed tagging results in the context of fisheries data to allow broader applications of our findings.

Materials and methods

PSAT tagging

Twenty-one PSATs (X-tag; Microwave Telemetry, Inc., Columbia, Maryland, USA) were deployed on adult bigeye tuna (mean ± standard deviation (SD): 131 ± 12 cm curved fork length (CFL)) between 2008 and 2010 aboard the longline vessel FV *Eagle Eye II* in the Northwest Atlantic (Table 1). Upon retrieval from a branch line, fish condition was assessed, and individuals that were undamaged and hooked in the gape were tagged either on board or alongside the boat with a long pole. Tags were tethered via monofilament to a nylon "umbrella" dart (Lutcavage et al. 1999; Wilson et al. 2005) and implanted in the dorsal musculature at the base of the second dorsal fin. Hooks were also removed. Round weight was visually estimated by the captain and senior crew members in 5 lb (1 lb = 0.454 kg) increments, and, for fish brought on board, CFL was measured to the nearest inch (1 in = 2.54 cm). When only weight (kg)

was available, it was used to estimate straight fork length (FL; cm) using the following length–mass equation: round weight = 2.396 × 10^{-5}(FL)$^{2.9774}$ (Parks et al. 1982). FL was then converted to CFL by the equation FL = CFL × 0.9728 (Salz et al. 2007). This conversion is based on data from Atlantic bluefin tuna, since no published data are available for Atlantic bigeye tuna and these two species have a similar body plan. PSATs were programmed to record relative light level, external temperature, and pressure (depth) every 2 min for 8 or 12 months. Physically recovered tags contained the full-resolution time series; otherwise data were subsampled by manufacturer routines for transmission through the Argos satellites. Transmitted formats included estimated sunrise and sunset times, daily minimum and maximum depths and temperatures, and depth and temperature records available at 15 min marks (0:00, 0:15, 0:30, 0:45) of the hour. All tags had a fail-safe release set at 4 days, which would indicate postrelease mortality or tag shedding. Returned data were imported into and managed through Tagbase, a freely available database system for electronic tags (Lam and Tsontos 2011).

Geolocation

Daily diel vertical behavior of bigeye tuna has been well documented (e.g., Musyl et al. 2003; Evans et al. 2008; Schaefer and Fuller 2010; Matsumoto et al. 2013b). We exploited this regularity in swimming pattern to derive inputs to a state-space model, Trackit, with sea surface temperature (SST) matching (Lam et al. 2010) for estimation of horizontal movement. Trackit utilizes a scanning algorithm that identifies solar events by examining differences in a time series of light values. This presents a problem for bigeye tuna, which typically spends daytime at deep depths and nighttime at shallow depths. Recorded light curves from this type of behavior show very little change in light intensity or a pattern where light increases near sunset instead of declining. We therefore developed a technique to use depth as a surrogate for light. A light-level proxy was constructed from depth records by excluding values deeper than 400 m and linearly rescaling them to the sensor range of relative light levels typical of implantable geolocating tags (e.g., Lotek Wireless LTD series, Wildlife Computers Mk series). Solar events were then identified using the Trackit scanning algorithm, and extreme outliers were removed prior to

running the model. We used daily maximum tag temperatures and 1° resolution weekly NOAA Optimum Interpolation SST V2 satellite imagery (Reynolds et al. 2007) as SST inputs for Trackit. For one tag, with a short deployment period (2010-17272; 18 days at liberty), a more basic model, Ukfsst (Lam et al. 2008), was used to estimate positions based on manufacturer-calculated geolocations and SST. Lastly, bathymetric correction was applied to all tracks to obtain the final position estimates (Galuardi et al. 2010).

Tag-recorded water column data

We defined depth and temperature records as day or night, based on local sunset and sunrise times calculated from estimated positions using the "sunriset" function in the R (version 2.15.2) package "maptools" (version 0.8-23; http://cran.r-project.org/web/packages/maptools). Data were summarized daily, and differences between SST and ambient temperatures (mean, minimum) recorded by a fish were also calculated.

Environmental parameters

To characterize potential bigeye tuna associations with the environment, we downloaded remote sensing and climatological data from NOAA CoastWatch ERDDAP (http://coastwatch.pfeg.noaa.gov/erddap). These include NASA Jet Propulsion Lab's Multiscale Ultra-high Resolution SST (global, 0.011° daily resolution), NOAA–NCDC Blended Sea Surface Winds Wind Stress (speed component, global, 0.25° daily resolution), Aviso Sea Surface Height Deviation (global, 0.25° daily resolution), Aqua MODIS Chlorophyll a (eastern United States, 0.0125° 8-day resolution), and dissolved oxygen (Garcia et al. 2010) and temperature (Locarnini et al. 2010) from World Ocean Atlas 2009, at 100 m intervals from 100 to 500 m (global, 1° monthly resolution). Bathymetric values were obtained from Smith and Sandwell Topography (0.0167° resolution, version 11.1). Along each track point, data were extracted for a neighborhood bounded by the 95% confidence region around a position estimate. A point value for the environmental variable was then obtained from averaging the values within a given neighborhood. Extraction routines are available through NOAA CoastWatch West Coast Regional Node (http://coastwatch.pfeg.noaa.gov/xtracto).

To estimate the position of the Gulf Stream, we used water column temperature data obtained from the Naval Oceanographic Office NCOM model (global, 0.125° 3-hour resolution), hosted by NOAA OceanNOMADS (http://ecowatch.ncddc.noaa.gov). We estimated the Gulf Stream position daily at noon as defined by the 12 °C isotherm at 400 m (Halkin and Rossby 1985).

Daytime deep scattering layer estimation

To investigate bigeye tuna utilization of the deep scattering layer (DSL) for foraging opportunities, we derived global maps of daytime DSL using remotely sensed datasets of NASA FLASHFlux solar insolation, INSOL (global, 0.25° 8-day resolution; http://neo.sci.gsfc.nasa.gov/Search.html?datasetId=CERES_INSOL_E) and diffuse attenuation coefficient at 490 nm, KD490 (global, 0.25° monthly resolution). KD490 and chlorophyll a, Case 1 water (global, 0.0417° monthly resolution) were obtained from GlobColour of European Space Agency (http://www.globcolour.info/data_access_nrt.html), which are derived from measurements across multiple sensors (MODIS, SeaWiFS, and MERIS). Monthly data were used to reduce gaps due to cloud cover.

We approximated irradiances at the top (10^9 photons·cm^{-2}·s^{-1}·nm^{-1} at 480 nm) and bottom (10^0 photons·cm^{-2}·s^{-1}·nm^{-1}) of daytime DSL from Frank and Widder (2002), who conducted in situ measurements of downwelling irradiance and distributions of various groups of DSL organisms in Oceanographer Canyon (40.3167°N,

68.133°W). Irradiances were converted into power per unit area (W·m^{-2}) according to the Planck relation to match the unit of INSOL. Depths at which these irradiances occurred were then calculated by applying the Beer–Lambert equation, $I_z = I_o e^{-kz}$, where I_z is the irradiance at depth (z), I_o is the surface irradiance, and k is the attenuation coefficient (KD490). Resulting maps of daytime DSL depths were available at an 8-day interval and 0.25° spatial resolution. Daytime DSL depths (top and bottom) were extracted along the track as previously described.

Generalized additive mixed models

We used generalized additive mixed models (GAMMs) to determine which factors influence daily vertical activity of bigeye tuna. Five different GAMMs were fit separately to the following measures of vertical activity ($\mathbf{R}_i$): daytime mean depth, nighttime mean depth, maximum depth, daytime mean temperature, and nighttime mean temperature. Since observations were repeated measures collected from the same individuals, we modeled individual fish as a random effect. We incorporated a number of explanatory variables as fixed effects: location, month, SST, temperature at 100 m intervals (100–500 m), dissolved oxygen at 100 m intervals, sea surface height deviation, surface wind speed, and daytime DSL depths. We accounted for spatial patterns by explicitly modeling location as a fixed effect.

GAMMs were constructed with the R package, "mgcv" (version 1.7-22; Wood 2006) using the Gaussian family with an identity–link function. Other than month, explanatory variables were modeled as continuous variables and smoothed. Smoothing functions were chosen automatically and evaluated manually using the "gam.check" function. We adopted the "top-down" model selection strategy (Diggle et al. 2002) by starting with a "beyond optimal" model, and subsequently dropping explanatory variables to arrive at the final model. The starting model is formulated as follows:

$$\mathbf{R}_i = S(\mathbf{Location}_i) + \mathbf{Month}_i + f_1(\mathbf{X}_1) + f_2(\mathbf{X}_2) + \ldots + f_j(\mathbf{X}_j) + \mathrm{Fish}_i \times b_i + \varepsilon$$

where $\mathbf{R}_i$ is the matrix of vertical activity for Fish$_i$ and $i = 1, \ldots, n$, where n represents the number of individual fish; S is a smoothing function for location; $\mathbf{Location}_i$ is the matrix of longitude and latitude for Fish$_i$; $\mathbf{Month}_i$ is the matrix of month of observation for Fish$_i$; $f_1 \ldots f_j$ are smoothing functions for environmental variable j, and $j = 1, \ldots,$ are the number of different environmental variables; $\mathbf{X}_1 \ldots \mathbf{X}_j$ are matrices of environmental variable j for Fish$_i$; $b_i \sim N(0, D)$ and $\varepsilon \sim N(0, \sigma^2)$, where D and σ^2 are variances, and $b_1 \ldots b_n$ and ε are independent.

We selected the final model by minimizing both the Akaike information criterion (AIC) and Bayesian information criterion (BIC) scores. Candidate predictors that were statistically significant at the $\alpha = 0.05$ level were retained during the selection process. Finally, we evaluated the models by checking diagnostic plots on fitted data and residuals (Fig. S2[1]).

Lunar influences on swimming depth

Correlation of diving depths (daily nighttime mean) with lunar illumination was investigated for tagged bigeye tuna that recorded data for more than two lunar cycles (approximately >59 days; $n = 5$). Concurrent data on fraction of the moon illuminated were obtained from the US Naval Observatory (http://aa.usno.navy.mil/data/docs/MoonFraction.php). We analyzed the correlation through

---

[1]Supplementary data are available with the article through the journal Web site at http://nrcresearchpress.com/doi/suppl/10.1139/cjfas-2013-0511.

the Pearson product–moment correlation coefficient between the two time series for each fish.

Fisheries data

To evaluate movements from tagged fish in relation to the bigeye tuna fishery in the Northwest Atlantic, we obtained conventional tag and fisheries data (Task II catch–effort; version Nov. 2012) from the ICCAT Secretariat (http://www.iccat.int/en/accesingdb.htm). We extracted longline (LL) data at the highest spatial resolution available for the Japanese (5° × 5°) and US (1° × 1°) fleets for the years 2000–2009 between 40°W and 85°W to calculate a mean catch per unit effort (CPUE; number of fish per 1000 hooks) at each station. CPUE was calculated only at stations with more than four sets during a given quarter. We chose this criterion to reduce bias due to too few samples at any station. Changes in distribution of quarterly CPUE were checked against 95% and 50% utilization distributions derived from PSAT tracks.

Results

Of the 21 X-tags deployed, 13 (62%) failed to report and 7 (33%) were shed prematurely and transmitted data via satellites. Fishermen recaptured one tag still attached to a fish before the programmed pop-off date and a nonreporting tag that failed to release on the pop-off date. A total of nine tags provided data records for 1–292 days (Table 1). No reliable physical measurements were available for the recaptured fish. Depth and temperature records showed no evidence of predation (e.g., uncharacteristically warm temperatures at depths >100 m) or postrelease mortality (e.g., constant bottom depth). Spatiotemporal correspondence of remotely sensed and tag-derived SSTs confirmed broad-scale accuracy of geolocation procedures.

Horizontal movements

Tagged bigeye tuna covered a wide geographical range between 0°N–40°N and 42°W–75°W, integrating regions of productive (Georges Bank, Guiana Basin, shelf off the Brazilian Amazon) and oligotrophic waters (Hatteras Plain: 31°N, 71°W). They also displayed some site fidelity in which five tags with >100 days at liberty reported close to tagging locations (Table 1). Given the months in which tagging occurred and the lengths of deployment, we derived position estimates for the months of October through May, and obtained positions for June through August from a single fish (Fig. 1). September was not represented.

Bigeye tuna showed high usage of the Hatteras Plain in the area southwest of Bermuda (Table 1; Fig. 1). Fish (2010-17271, 2010-17272, and 2010-17276) released within a 4-day period in late October at the Canyons (~40°N, 71°W) all swam south to the Hatteras Plain within 2–3 weeks (Figs. 1A–1C). In this area, fish either utilized waters northeast of the Bahamas (n = 5; Figs. 1A–1C, 1E) or continued south towards South America through the Caribbean Sea (n = 1; Fig. 1E) or the Atlantic Ocean off the Leeward Islands of the Lesser Antilles (n = 1; Fig. 1C). Two fish stayed along the South American coast between January and February (Figs. 1C and 1E). From February to April, fish moved northward towards areas south of the Gulf Stream (n = 2; Figs. 1D and 1F) or around the Hatteras Plain (n = 1; Fig. 1C). This northward shift continued through April and into the summer (n = 2). Gulf Stream margins (Fig. 2A) and Georges Bank (Fig. 2B) were utilized from June to August (n = 1). Tagging (n = 5) and recapture (n = 1) locations also suggest BET were north of the Gulf Stream from late summer to autumn (Table 1).

Oceanographic associations

With 98% of track points in areas of bottom depth >1000 m, tagged bigeye tuna stayed on the continental shelf break, on the continental slope, and in pelagic waters (Figs. 1 and 2). While surface chlorophyll associated with these environments varied from very low (<0.05 mg·m⁻³) to low (<0.4 mg·m⁻³), areas with enhanced (>1 mg·m⁻³) productivity can be found nearby (Figs. 2B and 2C). SST was between 12 and 29 °C (Fig. 3D). Temperature at 300 m was colder within the northern (40°N) and southern (5°N) extents of the tagged bigeye tuna latitudinal range than that in the subtropics (Fig. 3E). A high concentration of dissolved oxygen (>3 mL·L⁻¹) was present in the water column throughout the entire range (Fig. 3F). Bigeye tuna were also associated with highly dynamic Gulf Stream features (Fig. 2A).

Vertical activity

We observed deepest maximum depths south of 35°N (Fig. 3A), with an overall maximum depth of 1280 m and a temperature range of 2.7–28.2 °C (Table 2). Tagged bigeye tuna displayed consistent diel differences in depth and temperature distributions (Fig. 4; Table 2). Overall daytime depth (mean ± SD: 196 ± 92 m) was significantly (Student's t test; $p < 2 \times 10^{-16}$) deeper than nighttime depth (45 ± 29 m). Mean nighttime depth correlated significantly with lunar illumination (Table 2), but the level of correlation was only low to moderate (0.2–0.44), because deepening of nighttime depth either led or lagged the full moon. Temperature association was more variable and dependent on latitude (Figs. 5A and 5C). As bigeye tuna moved towards the Equator, peak temperature became warmer at night and cooler during the day. High usage of 17 °C strata was also evident at latitudes ≥20°N. Bigeye tuna experienced an ambient temperature 22 °C below SST, but the difference between SST and mean temperature was usually ≤4 °C (58% of data-days).

We observed several types of vertical movement in both transmitted and recovered time series, which were illustrated by recovered data from fish 2010-17271 (Fig. 6). Daytime dives punctuated deeper swimming activity (Figs. 6A–6C) or occurred frequently between 0 and 400 m (Fig. 6E). Excursions to the surface mixed layer became infrequent (Fig. 6D) when the fish traveled through the Nares Plain (Fig. 2D). Bigeye tuna switched between the following nighttime patterns, remaining (*i*) at the surface with occasional dives to 50–200 m (Figs. 6A and 6E), (*ii*) around the thermocline with few dives >100 m (Figs. 6B and 6D), and (*iii*) between the surface and thermocline (Fig. 6C). Shortly after being tagged, three fish (2010-17271, 2010-17272, and 2010-17276) remained above 100 m for a period of 5–7 days, a pattern exhibited when bigeye tuna associate with floating objects (Schaefer and Fuller 2002, 2005). Track positions indicated that these fish were near the Georges Bank canyons and New England seamounts (Fig. 1) and thus were not restricted by bathymetry.

Factors influencing daily vertical activity

None of the environmental factors examined for effects on daily vertical activity were significant in their predictions. Results from GAMMs identified location as the primary predictor of vertical activity. The effect of month was only important for mean nighttime temperature. Since seasonal temperature variations are most pronounced at the surface and mixed layer, bigeye tuna nighttime occupancy at shallow depths would reflect such variations. The best-fit models explained (adjusted R^2) 15%, 36%, 28%, 40%, and 80% of the variability for daytime mean depth, nighttime mean depth, maximum depth, daytime mean temperature, and nighttime mean temperature, respectively. Model predictions of daily vertical activity are shown in Figs. 5 and S1[1].

Daytime mean depth was deepest around 10°N–20°N and progressively shoaled at higher latitudes (Fig. 5A). Deepest maximum depth was found close to the South Atlantic Bight (Fig. S1[1]), between 20°N and 30°N and northwest of the area with deeper daytime mean depth. The use of daytime DSL depths (Fig. 3B) as proxies for potential prey field was not informative in predicting

Fig. 1. Tracks of tagged bigeye tuna (A) 2008-12975, 2010-14709, and 2010-17272; (B) 2010-17276; (C) 2010-17271; (D) 2010-14524; (E) 2010-14535; and (F) 2010-14526. Tagging locations: larger, thick-outlined circles; pop-off locations: triangles; contours of bottom depth ≤500 m: dotted lines. For the coloured version of this figure, refer to the Web site at http://www.nrcresearchpress.com/doi/full/10.1139/cjfas-2013-0511.
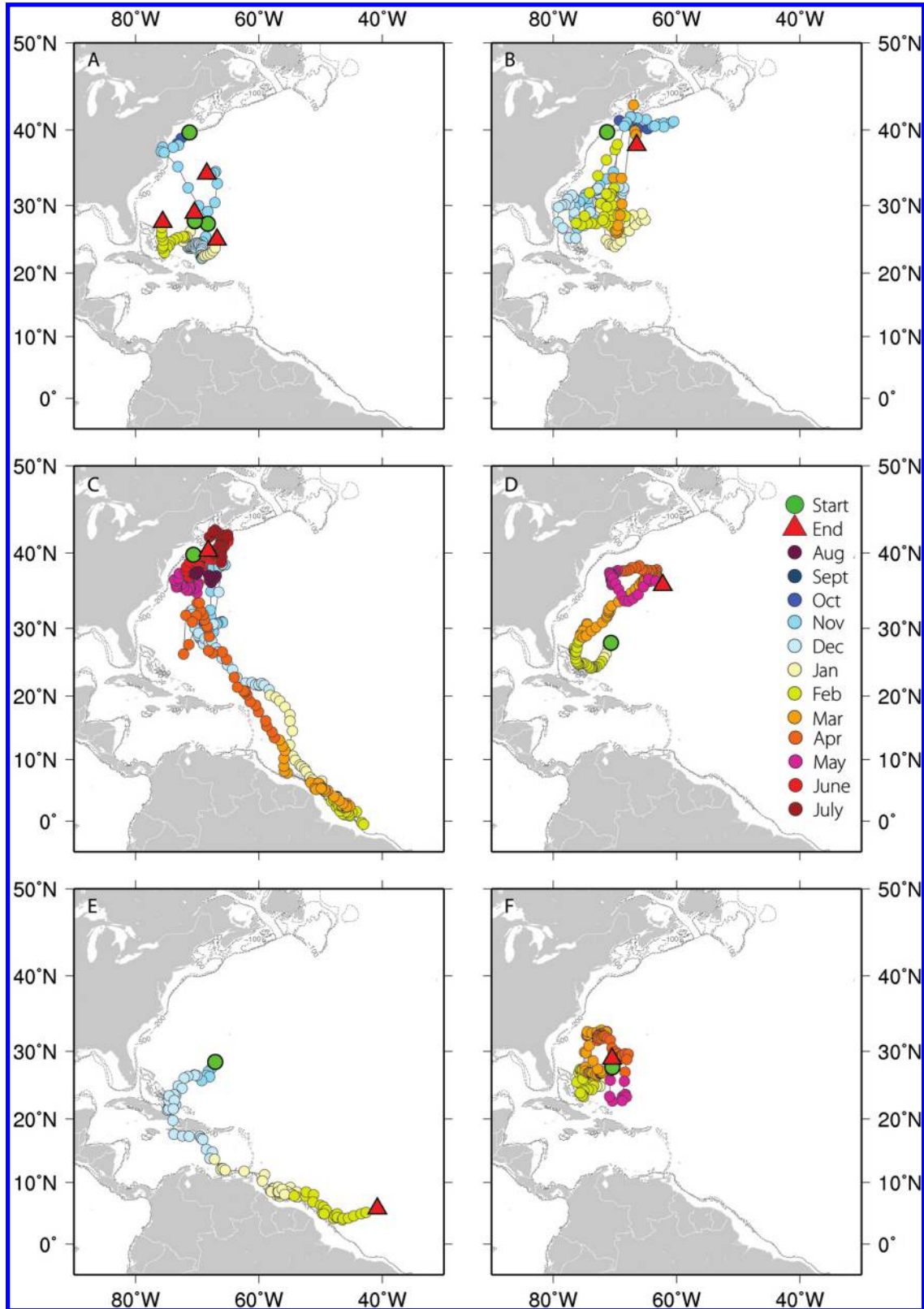
Fig. 2. Environmental conditions experienced by bigeye tuna. Chlorophyll *a* concentration is represented by satellite imagery (A, B: GlobColour of European Space Agency; C, D: NASA Aqua MODIS). Gulf Stream's north wall is shown in panels A and B for the beginning (light grey), midpoint (black), and end (grey) of the specified time period. Extracted track positions (circles) of fish 2010-17271 are also shown. For the coloured version of this figure, refer to the Web site at http://www.nrcresearchpress.com/doi/full/10.1139/cjfas-2013-0511.

Pagination not final (cite DOI) / Pagination provisoire (citer le DOI)
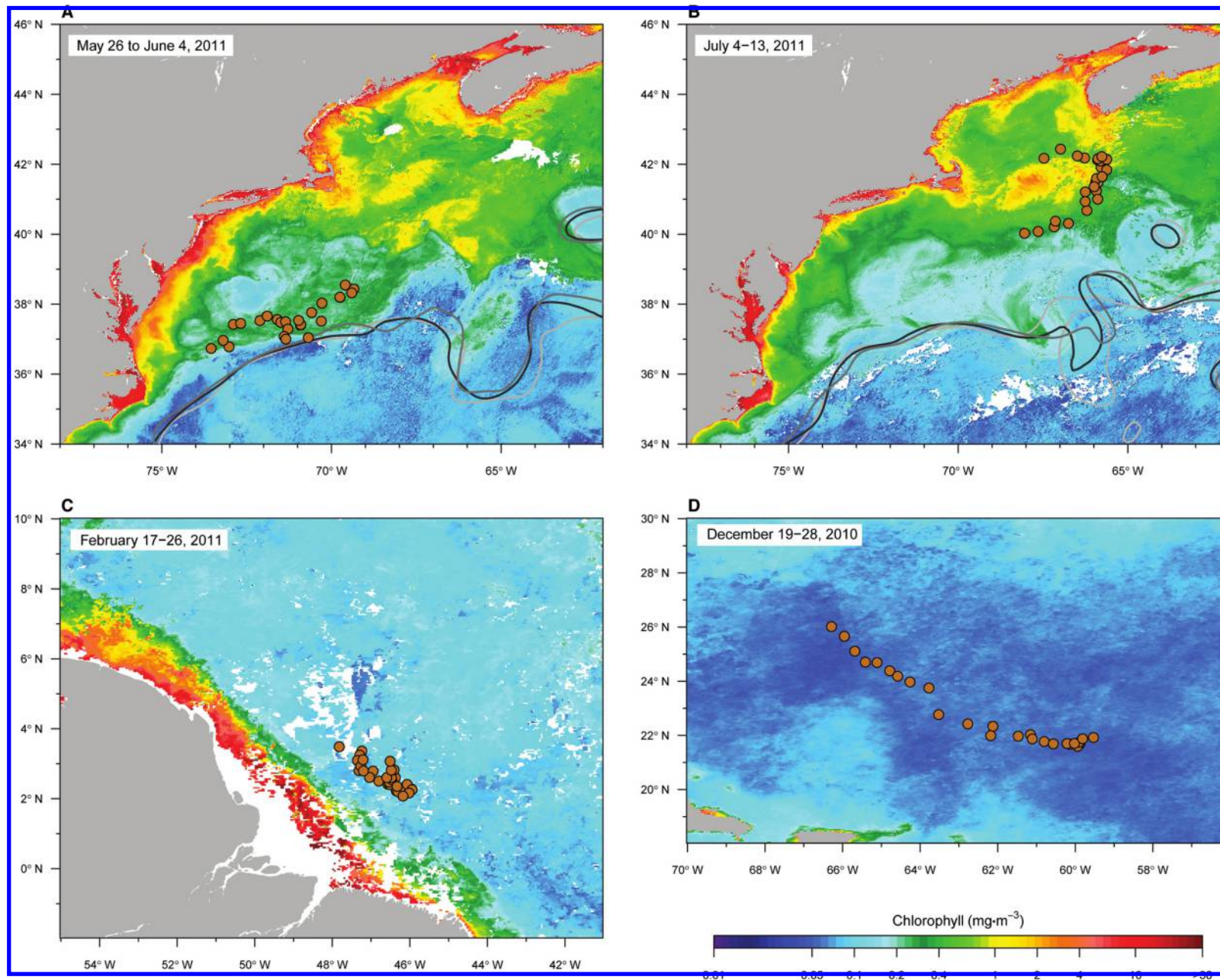
Fig. 3. Depths of bigeye tuna (A: mean daily maximum, C: mean daytime) and environmental parameters (B: top of daytime deep scattering layer, D: sea surface temperature, E: water column temperature at 300 m, F: dissolved oxygen concentration at 300 m) in a 1° × 1° grid. For the coloured version of this figure, refer to the Web site at http://www.nrcresearchpress.com/doi/full/10.1139/cjfas-2013-0511.
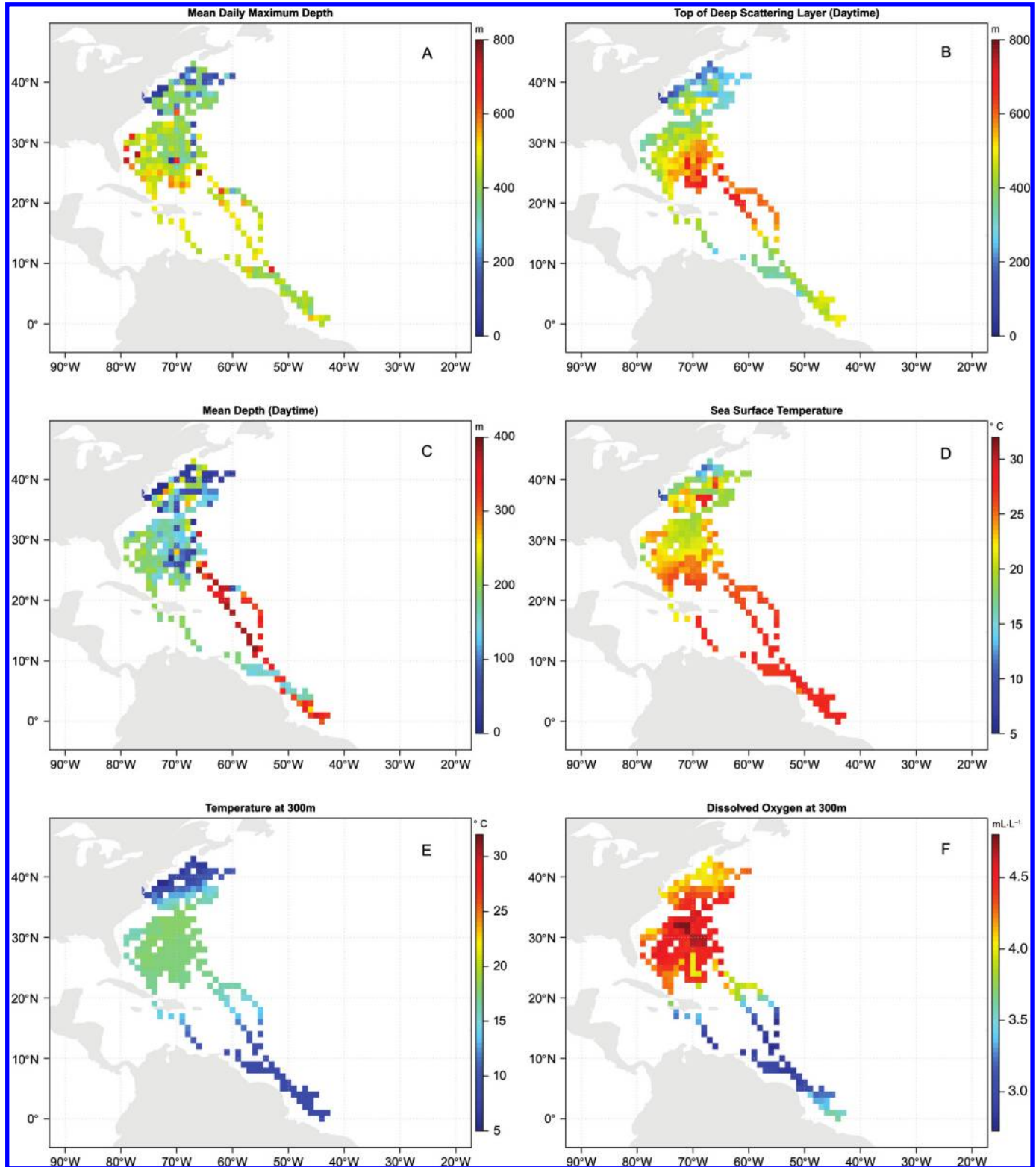
vertical activity, even though bigeye tuna presumably target DSL organisms (Josse et al. 1998; Dagorn et al. 2000; Matsumoto et al. 2013a). Nighttime mean depth was shallower than 100 m, with bigeye tuna staying close to the sea surface at >32°N (Fig. 5B).

Colder daytime mean temperature (<17 °C) was found at higher latitudes and around the Equator (Fig. 5C), while nighttime mean temperature followed a warming gradient from high to low latitudes (Fig. 5D).

Pagination not final (cite DOI) / Pagination provisoire (citer le DOI)

8

Can. J. Fish. Aquat. Sci. Vol. 71, 2014

Table 2. Summary of depth and temperature records of tagged bigeye tuna.

Tag ID	CFL (cm)	Data-days	Min. temp. (°C)	Max. temp. (°C)	Mean daily temp. range (°C)	Max. depth (m)	Mean daytime depth (m)	Mean nighttime depth (m)	Moon fraction correlation
2008-12975	136	36	14.2	26.2	8.1	522	169	40	NA
2010-14524	119	114	11.5	24.6	3.4	574	152	32	0.24*
2010-14526	122	103	15.7	26.4	4.3	585	171	28	0.44***
2010-14535	144	86	5.2	28.2	14.7	1081	151	49	0.38***
2010-14709[a]	119	19	15.7	24.1	6.1	614	422	71	NA
2010-17271[a]	148	292	2.7	28.0	13.9	844	258	58	0.20***
2010-17272	133	14	12.4	25.8	3.8	129	15	17	NA
2010-17276	148	134	3.9	25.8	6.8	1280	140	40	0.33***
Pooled daily data	—	—	2.7	28.2	9.4	1280	196	45	—

Note: *, $p < 0.01$; ***, $p < 0.0001$. CFL, curved fork length; NA, not applicable.
[a]Recovered physically.

Fig. 4. Cumulative frequencies (as percentages) of depth (A) and temperature (B) of tagged bigeye tuna ($n = 8$).

Tag performance

We observed a very low reporting rate (35%; $n = 20$; 15%–59%, binomial 95% probability confidence interval) as compared with the reporting rate (90%; $n = 31$; 81%–97%, bootstrapped 95% confidence interval) for bigeye tuna from a meta-analysis of four studies (Musyl et al. 2011). On a positive note, our tag retention (mean 117 days) is comparable to other mesopelagic species (96 days) and is much longer than bigeye tuna (9 days) utilizing tags from the same manufacturer (Musyl et al. 2011). The number of data-days transmitted were also much higher (mean of 70 data-days in Table 1 versus 40 data-days in Musyl et al. 2011 Mesopelagic II).

Given the size of adult bigeye tuna, risk of predation by sharks is likely lower than that of smaller species, such as American eels (Béguer-Pon et al. 2012) and Atlantic salmon (Lacroix 2014). Even when ingested, X-tags transmitted 65%–100% of their data after being expelled by the predators, a process that took 3–8 days (Béguer-Pon et al. 2012). While it is not possible to attribute failure in reporting to any particular cause, patterns in reporting rates for mesopelagic species are influenced by tag production year, depth, and temperature (Musyl et al. 2011). X-tags deployed in 2008 on Atlantic bluefin tuna experienced high nonreporting (Galuardi and Lutcavage 2012) as a result of a software problem present in the tag batch (Paul Howey, Microwave Telemetry, Inc., personal communication). In our study, the release mechanism on tag 2010-14709 failed, as the tag remained attached to a fish 197 days after the scheduled pop-off. This same tag also stopped data acquisition 19 days after the deployment (programmed for 365 days). System failure is difficult, if not impossible, to identify, as compromised tags may not communicate with satellites and are rarely recovered. In addition, repetitive diving of bigeye tuna (and similarly, bluefin tuna and swordfish) may stress tags to a greater extent than in other species. Manufacturers and users alike must contend with and factor in unpredictable tag performance and sources of failures, especially when PSATs are used in some studies to evaluate postrelease mortality.

Geolocation

Positions estimated by proprietary manufacturer software using times of sunrise and sunset can be sporadic and highly variable (Royer and Lutcavage 2009). This challenge is often accentuated by deep-diving species such as bigeye tuna (Gunn et al. 2005) and swordfish (Neilson et al. 2009). X-tag light sensors are optimized for capturing times of sunrise and sunset and cut off or saturate quickly at low and high light levels. Since gradual changes in light level are required for successful application of the Trackit model (Nielsen and Sibert 2007), geolocating recovered X-tags using light data has remained problematic.

Our novel use of depth for geolocation has allowed us to circumvent hardware limitations and utilize the wealth of recorded depth and temperature time series in a coherent statistical framework. Simulation results showed that measurements recorded as infrequently as 14.4 min apart are sufficient for running Trackit

Discussion

This study provides the first fisheries-independent information on horizontal and vertical habitat use of bigeye tuna in the Northwest Atlantic. Tagged fish moved primarily north to south and remained in pelagic waters. Bigeye tuna displayed typical diel swimming with deeper (>300 m) daytime depths and spent little time at shallow depths. At night, bigeye tuna remained within the surface mixed layer and exhibited several depth patterns that were not previously observed (Schaefer and Fuller 2002, 2005) or described (e.g., Fig. 6 in Musyl et al. 2003).

Fig. 5. Model predictions on daily mean daytime depth (A), nighttime depth (B), daytime temperature (C), and nighttime temperature (D) of bigeye tuna. For the coloured version of this figure, refer to the Web site at http://www.nrcresearchpress.com/doi/full/10.1139/cjfas-2013-0511.
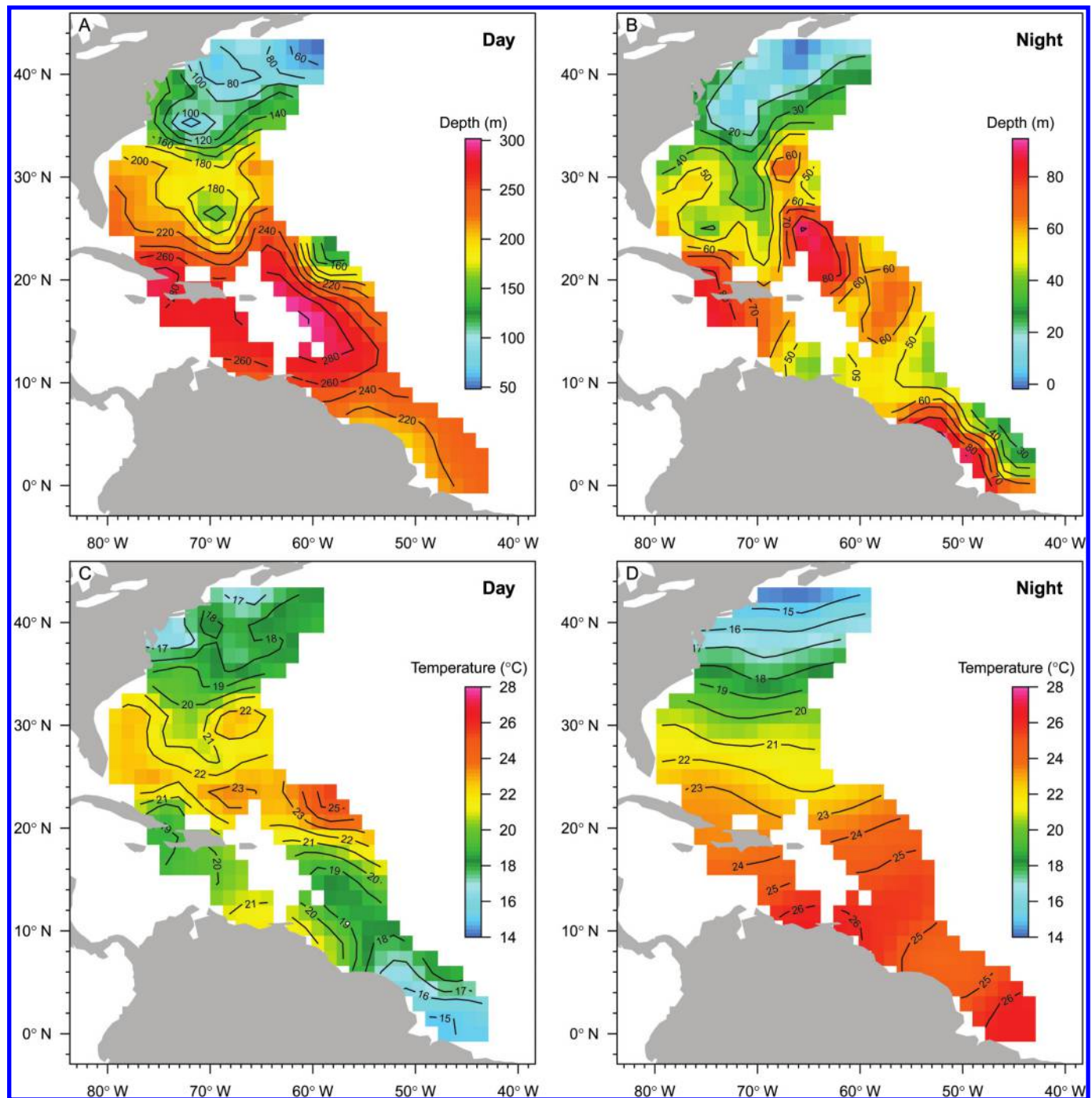
(Nielsen and Sibert 2007). This allows a PSAT with only transmitted data, sampling every 15 min, to be geolocated using our depth-based method.

Horizontal habitat

Despite a small sample size, tagged fish displayed a greater range of movements than the occasional, extended east–west movements undertaken by bigeye tuna in the Pacific (Evans et al. 2008; Schaefer and Fuller 2010). Tagged bigeye tuna showed directed northward movements in April towards the South and Mid-Atlantic. This coincides with the onset of northward migration by swordfish from the Caribbean to temperate waters for

foraging (Neilson et al. 2009). Even though two bigeye tuna traveled south and stayed within the potential spawning areas off Northeast Brazil, they did so between January and March, which is outside the known peak spawning period (June to August) for this area.

The bigeye tuna high-use area in the Hatteras Plain (within the Bermuda Triangle) is a transit region for swordfish, which had more restricted movement patterns north of 40°N and in the Caribbean (Neilson et al. 2009). Blue shark used waters mostly north of 30°N and near the Gulf Stream (Campana et al. 2011). Other shark species, such as the oceanic whitetip (Howey-Jordan et al.

Pagination not final (cite DOI) / Pagination provisoire (citer le DOI)

10

Can. J. Fish. Aquat. Sci. Vol. 71, 2014

Fig. 6. Time series of depth and temperature for bigeye tuna 2010-17271 near latitudes (A) 28.9°N, (B) 17.5°N, (C) 2.5°N, (D) 22.0°N, and (E) 37.5°N. For the coloured version of this figure, refer to the Web site at http://www.nrcresearchpress.com/doi/full/10.1139/cjfas-2013-0511.
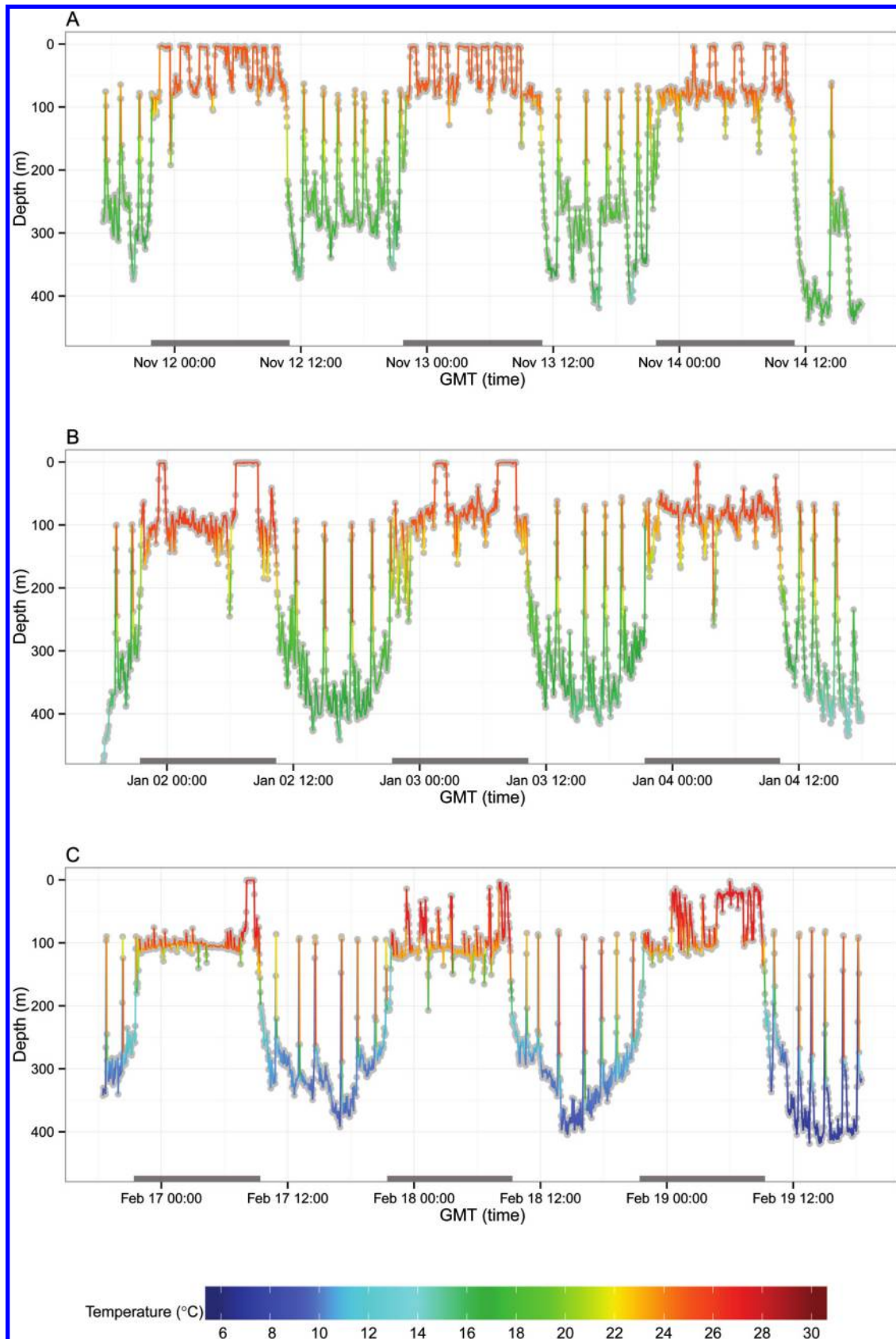
Fig. 6 (*concluded*).
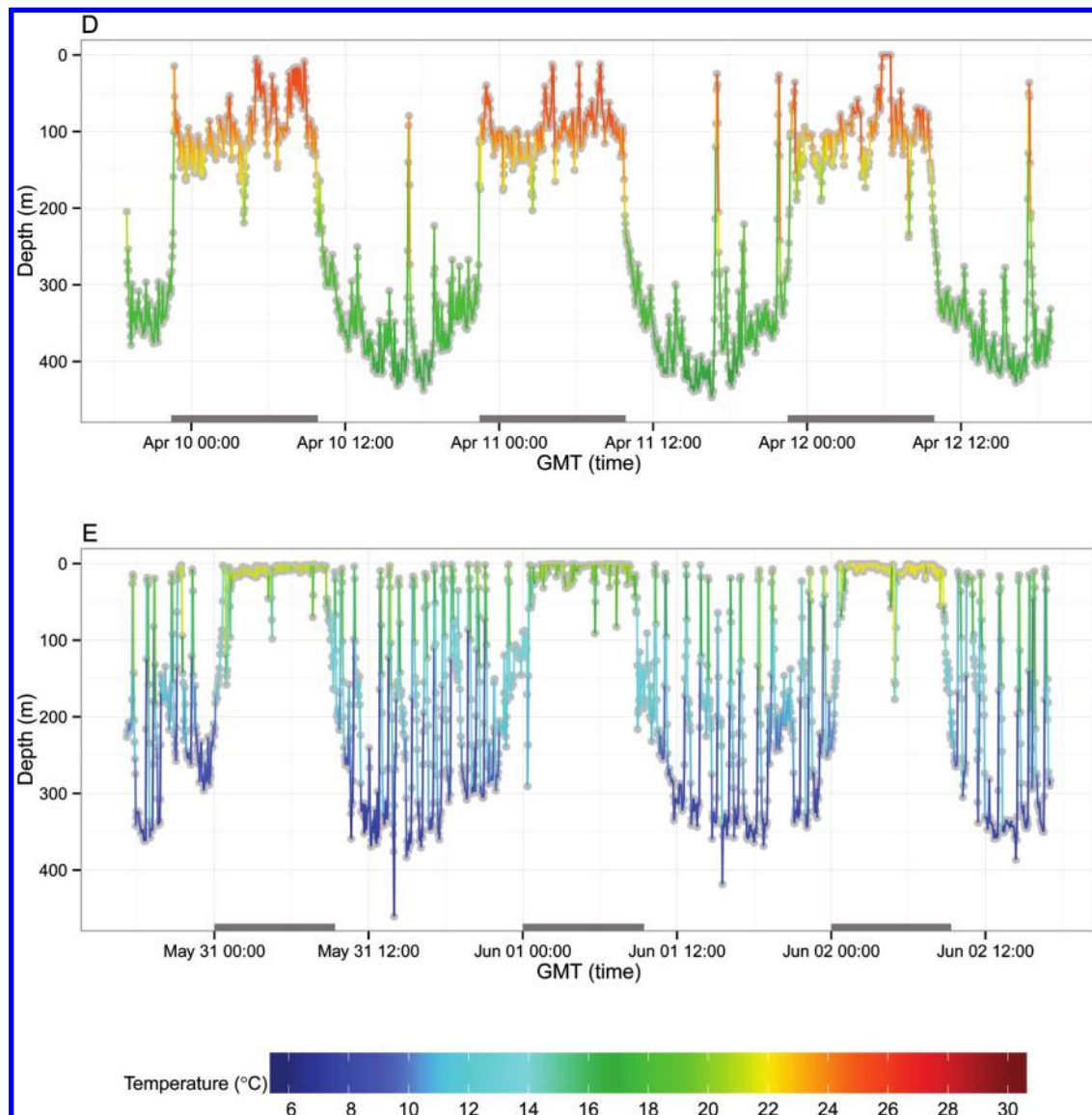
2013), inhabit this area, but these sharks primarily utilize surface waters (<40 m) and generally overlap with bigeye tuna in the water column only at night. Adult and juvenile bluefin tuna also overlap with bigeye tuna in this area, but show much greater use of the Mid-Atlantic Bight, Gulf Stream, and Gulf of Mexico (Wilson et al. 2005; Sibert et al. 2006; Walli et al. 2009; Galuardi et al. 2010; Galuardi and Lutcavage 2012). Further north, fisheries information indicates these two tuna species overlap in the Scotian shelf region, but bigeye tuna were more associated with warmer offshore water of Gulf Stream origin, while bluefin occupied cooler inshore water (Neilson et al. 2005). These observations suggest a degree of horizontal and vertical habitat partitioning by bigeye tuna and other pelagic species in the Northwest Atlantic.

Fisheries considerations

Horizontal movements of tagged bigeye tuna agreed with patterns observed in conventional tag returns and quarterly changes in CPUE distribution from US (USLL) and Japanese (JPLL) longline fisheries (Fig. 7). Among the 12 conventional tags originating from or terminating in the Northwest Atlantic, two deployed off West

Africa were recaptured after >2 years in the Caribbean, and one deployed off the Mid-Atlantic Bight was recaptured 9 years later in the Central South Atlantic. The remaining tags, at liberty for an average of 17 months, were located off the shelf around the Mid-Atlantic and New England, similar to our results.

High CPUE JPLL areas were found further east than utilization distributions of our tracked bigeye tuna (Fig. 7). However, JPLL showed high CPUE near South America between 5°N and 10°N, particularly in the first quarter (Q1, December–February), when two tagged fish moved into this region (Figs. 1C and 1E). For USLL, fishing activity mostly took place near the US and Canadian exclusive economic zones. Bigeye tuna utilization distributions generally overlapped with high USLL CPUE areas, with an exception of the areas east of the Scotian shelf, where we did not observe any fish movements. High CPUE was found throughout the year in the western part of the Hatteras Plain high-use area (Fig. 7). Movement of tagged fish followed the seasonal north–south shift in distribution of USLL CPUE. Areas with moderate to high CPUE were found between 10°N and 30°N in winter (Q1, December–February), spread north in spring (Q2, March–May), and finally concentrated north of 25°N, off the continental shelf between Cape Hatteras

Fig. 7. Distribution of longline catch per unit effort (number of bigeye tuna caught per 1000 hooks) by quarters (Q1: December–February, Q2: March–May, Q3: June–August, Q4: September–November) for the United States (vertical scale) and Japan (horizontal scale) between 2000 and 2009. Utilization distribution contours (95%, red (gray in black and white version); 50%, black) of tagged tuna are also shown, and the number of individuals (*n*) is noted. For the coloured version of this figure, refer to the Web site at http://www.nrcresearchpress.com/doi/full/10.1139/cjfas-2013-0511.
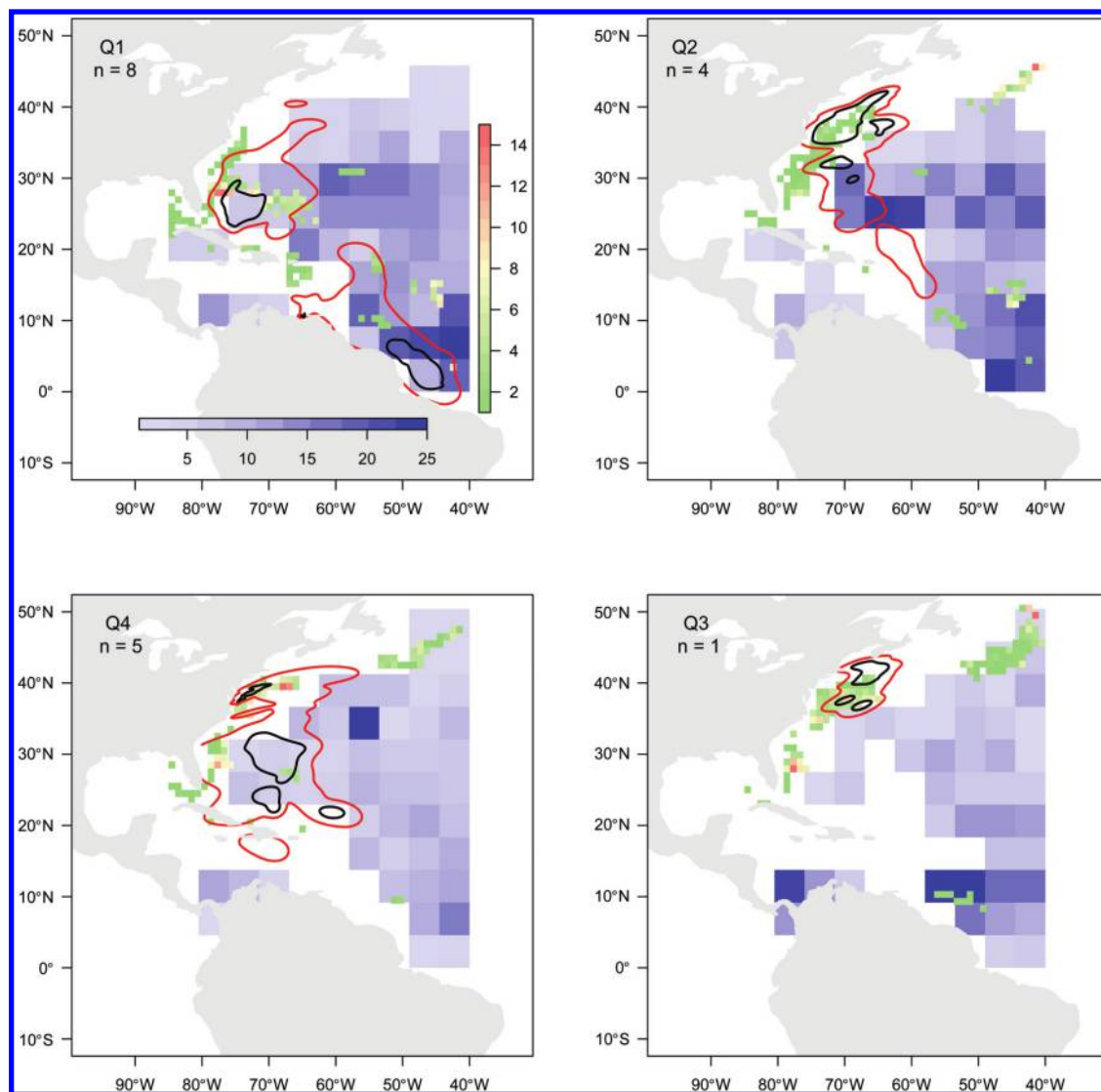
and Cape Cod, in summer (Q3, June–August) and fall (Q4, September–November). Finally, during winter (Q4 to Q1), higher CPUE areas shifted south from >40°N towards the tropics.

In the basin-wide context, catch in the Northwest Atlantic LL fishery constitutes a small proportion of the total bigeye tuna catch. Japanese and Chinese Taipei LL fleets in the Central Atlantic and baitboat and purse seine fisheries in the West Atlantic account for the majority of catch (Anonymous 2013). As our models suggest, geographic location plays a key role in structuring vertical habitat utilization and consequently affects vulnerability of bigeye tuna. With such spatial specificity, fisheries-independent information in the high-catch areas will be required to better understand fishery interactions.

Temperature habitat and thermoregulation

When fisheries-dependent data were used to characterize the temperature habitat for bigeye tuna in the Pacific (Bigelow et al. 2002), high CPUE was mostly found in areas where the 15 °C isotherm occurs within the top 200 m of the water column (Hampton et al. 1998), although fishing practices may bias the inference.

Archival tags provide a more complete description of ambient water temperature range and usage. Similar to bigeye tuna in the Pacific, tagged fish rarely experienced temperatures below 10 °C or above 28 °C. Moreover, the lowest temperatures were experienced by the larger fish (Table 1), consistent with earlier findings (Pelczarski and Kêdra 2005; Arrizabalaga et al. 2008; Song et al. 2009). While bigeye tuna (49–72 cm FL at release; *n* = 28) off southwestern Japan reduced their nighttime surface activity (<30 m) when surface temperature was above 28 °C (Matsumoto et al. 2013b), our temperature data rarely reached that high. Daytime temperatures of bigeye tuna varied substantially by location between 0°N and 25°N (Fig. 5), while depth usage was fairly consistent (>200 m) throughout the same area. This suggests that temperature habitat simply reflects where a fish is in the water column, as driven by foraging (Schaefer and Fuller 2002) or other biological activities. In addition, the effects of location, other than just cohort (or body size), should be considered in model representations of temperature habitat (Lehodey et al. 2010).
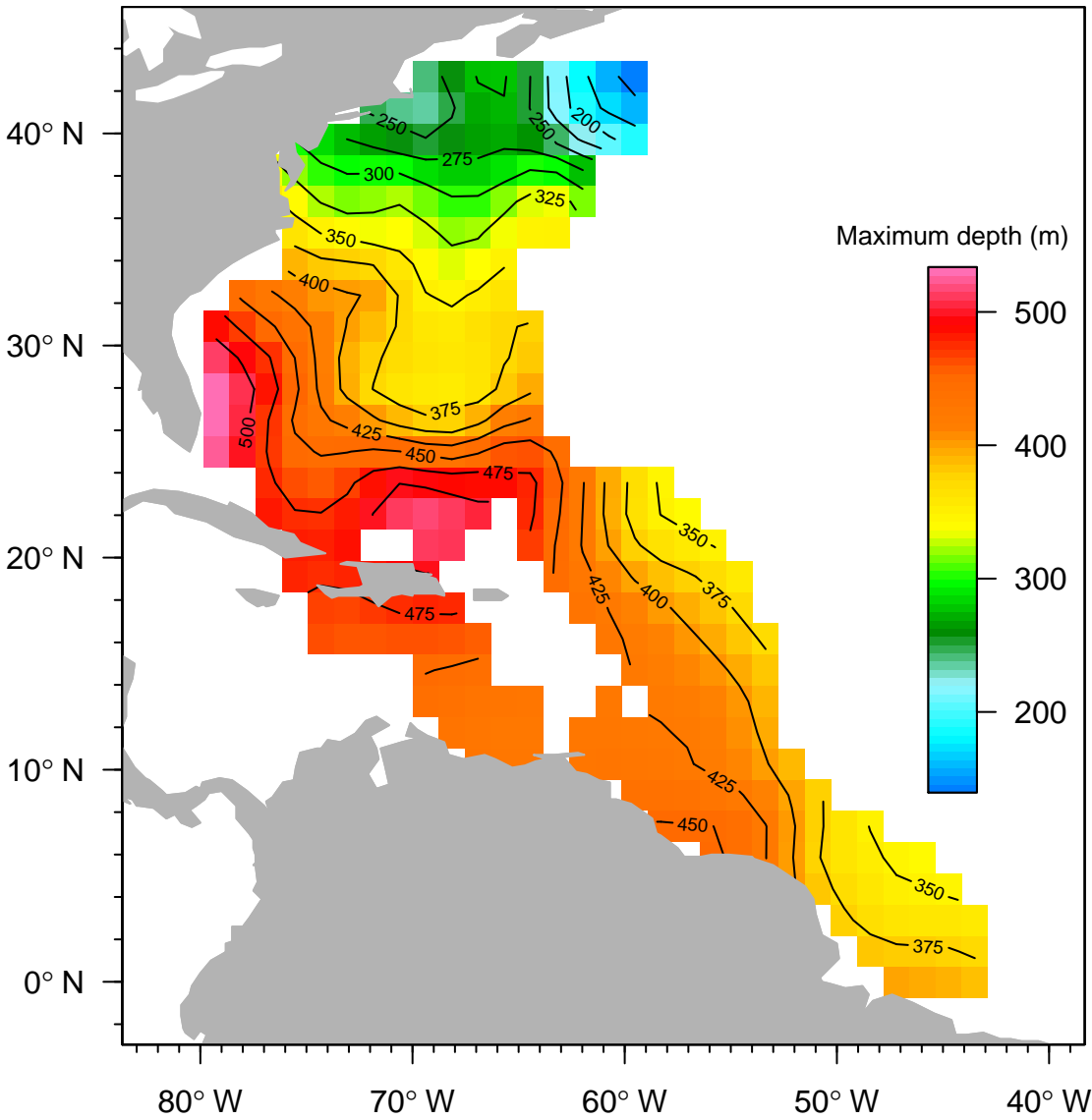
overwintering grounds of blue sharks in the Northwest Atlantic. PloS ONE, **6**(2): e16854. doi:10.1371/journal.pone.0016854. PMID:21373198.

Carey, F.G., and Teal, J.M. 1966. Heat conservation in tuna fish muscle. Proc. Natl. Acad. Sci. U.S.A. **56**(5): 1464–1469. doi:10.1073/pnas.56.5.1464. PMID:16591392.

Cavérivière, A., Conaud, F., and de Sainte Claire, E.S. 1976. Distribution et abondance des larves de thonides dans l'Atlantique tropico-oriental etude des donnees de 1963 a 1974 Doc. Scient. Centre Rech. Océanogr. Abidjan, **7**(2): 49–70.

Cayré, P., Amon Kothias, J.B., Diouf, T., and Stretta, J.M. 1991. Biología de los atunes. Collect. Vol. Sci. Pap. ICCAT, **37**(1): 169–291.

Chapman, E.W., Jørgensen, C., and Lutcavage, M.E. 2011. Atlantic bluefin tuna (*Thunnus thynnus*): a state-dependent energy allocation model for growth, maturation, and reproductive investment. Can. J. Fish. Aquat. Sci. **68**(11): 1934–1951. doi:10.1139/f2011-109.

Dagorn, L., Bach, P., and Josse, E. 2000. Movement patterns of large bigeye tuna (*Thunnus obesus*) in the open ocean, determined using ultrasonic telemetry. Mar. Biol. **136**(2): 361–371. doi:10.1007/s002270050694.

Diggle, P.J., Heagerty, P., Liang, K.-Y., and Zeger, S.L. 2002. Analysis of longitudinal data. Oxford University Press, Oxford, England.

dos Santos, R.A., and Haimovici, M. 2000. The Argentine short-finned squid *Illex argentinus* in the food webs of southern Brazil. Sarsia, **85**(1): 49–60.

Duarte-Neto, P., Higa, F.M., and Lessa, R.P. 2012. Age and growth estimation of bigeye tuna, *Thunnus obesus* (Teleostei: Scombridae) in the southwestern Atlantic. Neotrop. Ichthyol. **10**(1): 149–158. doi:10.1590/S1679-62252012000100014.

Durand, J.D., Collet, A., Chow, S., Guinand, B., and Borsa, P. 2005. Nuclear and mitochondrial DNA markers indicate unidirectional gene flow of Indo-Pacific to Atlantic bigeye tuna (*Thunnus obesus*) populations, and their admixture off southern Africa. Mar. Biol. **147**(2): 313–322. doi:10.1007/s00227-005-1564-2.

Evans, K., Langley, A., Clear, N.P., Williams, P., Patterson, T., Sibert, J., Hampton, J., and Gunn, J.S. 2008. Behaviour and habitat preferences of bigeye tuna (*Thunnus obesus*) and their influence on longline fishery catches in the western Coral Sea. Can. J. Fish. Aquat. Sci. **65**(11): 2427–2443. doi:10.1139/F08-148.

FAO. 2002. The living marine resources of the Western Central Atlantic Volume 1: Introduction, molluscs, crustaceans, hagfishes, sharks, batoid fishes, and chimaeras. FAO Species Identification Guide for Fishery Purposes and American Society of Ichthyologists and Herpetologists Special Publication No. 5. Food and Agriculture Organization of the United Nations, Rome.

Frank, T.M., and Widder, E.A. 2002. Effects of a decrease in downwelling irradiance on the daytime vertical distribution patterns of zooplankton and micronekton. Mar. Biol. **140**(6): 1181–1193. doi:10.1007/s00227-002-0788-7.

Galuardi, B., and Lutcavage, M. 2012. Dispersal routes and habitat utilization of juvenile Atlantic bluefin tuna, *Thunnus thynnus*, tracked with Mini PSAT and archival tags. PloS ONE, **7**(5): e37829. doi:10.1371/journal.pone.0037829. PMID:22629461.

Galuardi, B., Royer, F., Golet, W., Logan, J., Neilson, J., and Lutcavage, M. 2010. Complex migration routes of Atlantic bluefin tuna (*Thunnus thynnus*) question current population structure paradigm. Can. J. Fish. Aquat. Sci. **67**(6): 966–976. doi:10.1139/F10-033.

Garcia, H.E., Locarnini, R.A., Boyer, T.P., Antonov, J.I., Baranova, O.K., Zweng, M.M., and Johnson, D.R. 2010. World Ocean Atlas 2009. Vol. 3: Dissolved oxygen, apparent oxygen utilization, and oxygen saturation. US Government Printing Office, Washington, D.C.

Gonzalez, E.G., Beerli, P., and Zardoya, R. 2008. Genetic structuring and migration patterns of Atlantic bigeye tuna, *Thunnus obesus* (Lowe, 1839). BMC Evol. Biol. **8**: 252. doi:10.1186/1471-2148-8-252. PMID:18798987.

Gorni, G.R., Goitein, R., and de Amorim, A.F. 2013. Description of diet of pelagic fish in the southwestern Atlantic, Brazil. Biotaneo Tropica, **13**(1): 61–69. doi:10.1590/S1676-06032013000100006.

Graham, J.B., and Dickson, K.A. 2001. Anatomical and physiological specializations for endothermy *In* Tuna: physiology, ecology and evolution. *Edited by* B.A. Block and E.D. Stevens. Academic Press, San Diego, Calif. pp. 121–165.

Gunn, J., Hampton, J., Evans, K., Clear, N., Patterson, T., Bigelow, K., Langley, A., Leroy, B., Williams, P., Miyabe, N., Sibert, J., Bestley, S., and Hartmann, K. 2005. Migration and habitat preferences of bigeye tuna on the east coast of Australia. Australian Government Fisheries Research and Development Corporation.

Halkin, D., and Rossby, T. 1985. The structure and transport of the Gulf Stream at 73°W. J. Phys. Oceanogr. **15**(11): 1439–1452. doi:10.1175/1520-0485(1985)015<1439:TSATOT>2.0.CO;2.

Hampton, J., Bigelow, K., and Labelle, M. 1998. Effect of longline fishing depth, water temperature and dissolved oxygen on bigeye tuna (*Thunnus obesus*) abundance indices. Standing Committee Tuna and Billfish Working Group Report.

Holland, K.N., and Sibert, J.R. 1994. Physiological thermoregulation in bigeye tuna, *Thunnus obesus*. Environ. Biol. Fishes, **40**(3): 319–327. doi:10.1007/BF00002520.

Holland, K.N., Brill, R.W., Chang, R.K.C., Sibert, J.R., and Fournier, D.A. 1992. Physiological and behavioural thermoregulation in bigeye tuna (*Thunnus obesus*). Nature, **358**(6385): 410–412. doi:10.1038/358410a0. PMID:1641023.

Howey-Jordan, L.A., Brooks, E.J., Abercrombie, D.L., Jordan, L.K.B., Brooks, A., Williams, S., Gospodarczyk, E., and Chapman, D.D. 2013. Complex movements, philopatry and expanded depth range of a severely threatened pelagic shark, the oceanic whitetip (*Carcharhinus longimanus*) in the western North Atlantic. PloS ONE, **8**(2): e56588. doi:10.1371/journal.pone.0056588. PMID:23437180.

ICCAT. 2006. ICCAT Manual. International Commission for the Conservation of Atlantic Tunas.

Josse, E., Bach, P., and Dagorn, L. 1998. Simultaneous observations of tuna movements and their prey by sonic tracking and acoustic surveys. Hydrobiologia, **372**: 61–69.

Lacroix, G.L. 2014. Large pelagic predators could jeopardize the recovery of endangered Atlantic salmon. Can. J. Fish. Aquat. Sci. **71**(3): 343–350. doi:10.1139/cjfas-2013-0458.

Lam, C.H., and Tsontos, V.M. 2011. Integrated management and visualization of electronic tag data with Tagbase. PloS ONE, **6**(7): e21810. doi:10.1371/journal.pone.0021810. PMID:21750734.

Lam, C.H., Nielsen, A., and Sibert, J.R. 2008. Improving light and temperature based geolocation by unscented Kalman filtering. Fish. Res. **91**(1): 15–25. doi:10.1016/j.fishres.2007.11.002.

Lam, C.H., Nielsen, A., and Sibert, J.R. 2010. Incorporating sea-surface temperature to the light-based geolocation model TrackIt. Mar. Ecol. Prog. Ser. **419**: 71–84. doi:10.3354/meps08862.

Lehodey, P., Senina, I., Sibert, J., Bopp, L., Calmettes, B., Hampton, J., and Murtugudde, R. 2010. Preliminary forecasts of Pacific bigeye tuna population trends under the A2 IPCC scenario. Prog. Oceanogr. **86**(1–2): 302–315. doi:10.1016/j.pocean.2010.04.021.

Locarnini, R.A., Mishonov, A.V., Antonov, J.I., Boyer, T.P., Garcia, H.E., Baranova, O.K., Zweng, M.M., and Johnson, D.R. 2010. World Ocean Atlas 2009. Vol. 1: Temperature. US Government Printing Office, Washington, D.C.

Logan, J.M., Toppin, R., Smith, S., Galuardi, B., Porter, J., and Lutcavage, M.E. 2012. Contribution of cephalopod prey to the diet of large pelagic fish predators in the central North Atlantic Ocean. Deep Sea Res. Part II Top. Stud. Oceanogr. **95**: 74–82. doi:10.1016/j.dsr2.2012.06.003.

Lutcavage, M.E., Brill, R.W., Skomal, G.B., Chase, B.C., and Howey, P.W. 1999. Results of pop-up satellite tagging of spawning size class fish in the Gulf of Maine: do North Atlantic bluefin tuna spawn in the mid-Atlantic? Can. J. Fish. Aquat. Sci. **56**(2): 173–177. doi:10.1139/f99-016.

Malte, H., Larsen, C., Musyl, M., and Brill, R. 2007. Differential heating and cooling rates in bigeye tuna (*Thunnus obesus* Lowe): a model of non-steady state heat exchange. J. Exp. Biol. **210**(15): 2618–2626. doi:10.1242/jeb.003855. PMID:17644676.

Marchal, E., Gerlotto, F., and Stequert, B. 1993. On the relationship between scattering layer, thermal structure and tuna abundance in the Eastern Atlantic equatorial current system. Oceanol. Acta, **16**(3): 261–272.

Martínez, P., González, E.G., Castilho, R., and Zardoya, R. 2006. Genetic diversity and historical demography of Atlantic bigeye tuna (*Thunnus obesus*). Mol. Phylogenet. Evol. **39**(2): 404–416. doi:10.1016/j.ympev.2005.07.022. PMID:16188460.

Matsumoto, T., and Miyabe, N. 2002. Preliminary report on the maturity and spawning of bigeye tuna *Thunnus obesus* in the central Atlantic Ocean. Collect. Vol. Sci. Pap. ICCAT, **54**(1): 246–260.

Matsumoto, T., Saito, H., and Miyabe, N. 2005. Swimming behavior of adult bigeye tuna using pop-up tags in the central Atlantic Ocean. Collect. Vol. Sci. Pap. ICCAT, **57**(1): 151–170.

Matsumoto, T., Kitagawa, T., and Kimura, S. 2013*a*. Considerations on diving patterns of bigeye tuna *Thunnus obesus* based on archival tag data. Fish. Sci. **79**(1): 39–46. doi:10.1007/s12562-012-0571-8.

Matsumoto, T., Kitagawa, T., and Kimura, S. 2013*b*. Vertical behavior of bigeye tuna (*Thunnus obesus*) in the northwestern Pacific Ocean based on archival tag data. Fish. Oceanogr. **22**(3): 234–246. doi:10.1111/fog.12017.

Maunder, M.N., Hinton, M.G., Bigelow, K.A., and Langley, A.D. 2006. Developing indices of abundance using habitat data in a statistical framework. Bull. Mar. Sci. **79**(3): 545–559.

Moiseev, S.I. 1991. Observation of the vertical distribution and behavior of nektonic squids using manned submersibles. Bull. Mar. Sci. **49**(1–2): 446–456.

Musyl, M.K., Brill, R.W., Boggs, C.H., Curran, D.S., Kazama, T.K., and Seki, M.P. 2003. Vertical movements of bigeye tuna (*Thunnus obesus*) associated with islands, buoys, and seamounts near the main Hawaiian Islands from archival tagging data. Fish. Oceanogr. **12**(3): 152–169. doi:10.1046/j.1365-2419.2003.00229.x.

Musyl, M.K., Domeier, M.L., Nasby-Lucas, N., Brill, R.W., McNaughton, L.M., Swimmer, J.Y., Lutcavage, M.S., Wilson, S.G., Galuardi, B., and Liddle, J.B. 2011. Performance of pop-up satellite archival tags. Mar. Ecol. Prog. Ser. **433**: 1–28. doi:10.3354/meps09202.

Neilson, J.D., Stone, H.S., and Carruthers, E.H. 2005. Development of the Canadian fishery for bigeye tuna (*Thunnus obesus*) from 1994 to 2002. Collect. Vol. Sci. Pap. ICCAT, **58**(1): 268–282.

Neilson, J.D., Smith, S., Royer, F., Paul, S.D., Porter, J.M., and Lutcavage, M. 2009. Investigations of horizontal movements of Atlantic swordfish using pop-up satellite archival tags. *In* Tagging and tracking of marine animals with electronic devices. *Edited by* J.L. Nielsen, H. Arrizabalaga, N. Fragoso, A. Hobday, M. Lutcavage, and J. Sibert. Springer. pp. 145–159.

Nielsen, A., and Sibert, J.R. 2007. State-space model for light-based tracking of marine animals. Can. J. Fish. Aquat. Sci. **64**(8): 1055–1068. doi:10.1139/f07-064.

Pallarés, P., Pereira, P., Miyabe, N., and Fonteneau, A. 1996. Atlantic bigeye tuna: overview of present knowledge (November 1996). *In* Proceedings of the
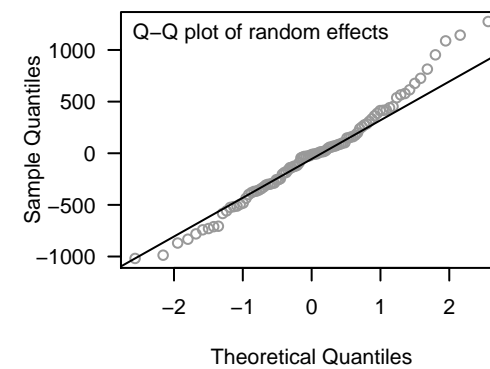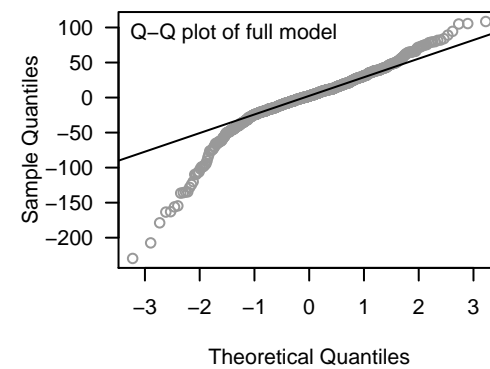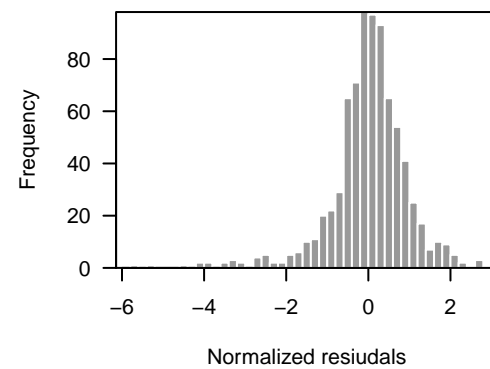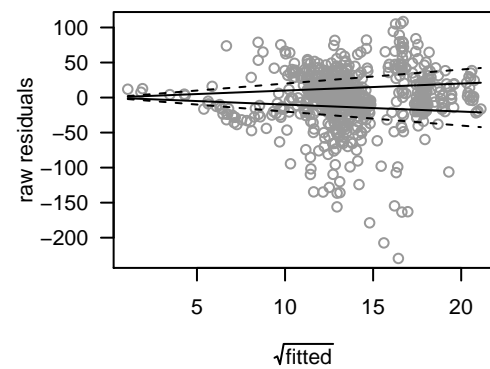
First World Meeting on Bigeye Tuna. *Edited by* R.B. Deriso, W.H. Bayliff, and N.J. Webb. pp. 20–80.

Parks, W., Bard, F.X., Cayré, P., Kume, S., and Santos Guerra, A. 1982. Length–weight relationships for bigeye tuna captured in the Eastern Atlantic Ocean Collect. Vol. Sci. Pap. ICCAT, **17**(1): 214–225.

Pelczarski, W., and Kędra, M. 2005. The impact of hydrological conditions on the catch results of bigeye tuna in Polish longline fishing. Collect. Vol. Sci. Pap. ICCAT, **58**(1): 253–267.
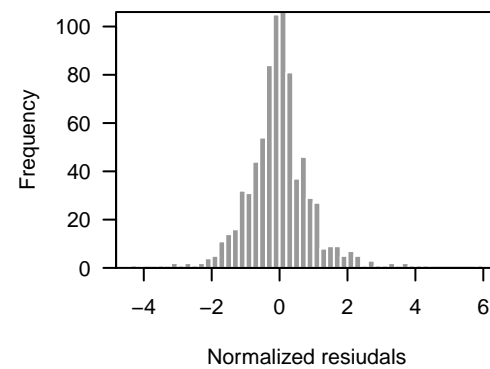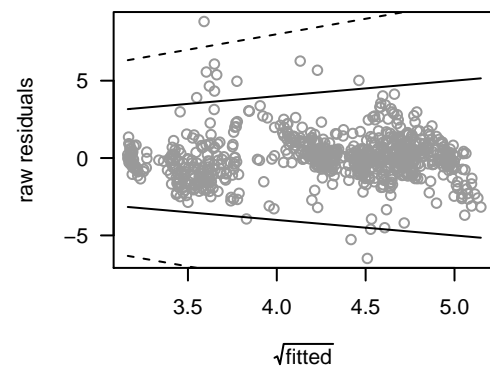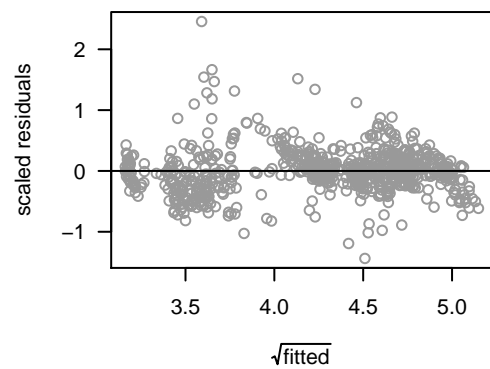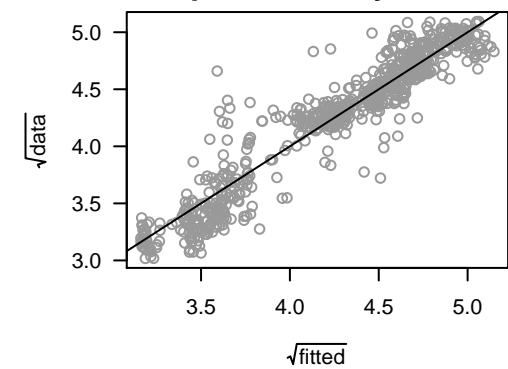
Reynolds, R.W., Smith, T.M., Liu, C., Chelton, D.B., Casey, K.S., and Schlax, M.G. 2007. Daily high-resolution-blended analyses for sea surface temperature. J. Clim. **20**(22): 5473–5496. doi:10.1175/2007JCLI1824.1.

Royer, F., and Lutcavage, M. 2009. Positioning pelagic fish from sunrise and sunset times: complex observation errors call for constrained, robust modeling. *In* Tagging and tracking of marine animals with electronic devices. *Edited by* J.L. Nielsen, H. Arrizabalaga, N. Fragoso, A. Hobday, M. Lutcavage, and J. Sibert. Springer. pp. 323–341.

Rudomiotkina, G.P. 1983. Areas, periods and conditions of bigeye tuna, *Thunnus obesus* (Lowe), spawning in the tropical part of the Atlantic Ocean. Collect. Vol. Sci. Pap. ICCAT, **18**(2): 355–362.

Salz, J.F., Van Voorhees, D., Brown, C., Desfosse, J., Schulze-Haugen, M., and Rogers, C. 2007. Large pelagics survey bluefin tuna length validation assessment. Collect. Vol. Sci. Pap. ICCAT, **60**(4): 1035–1056.

Satoh, K., Yokawa, K., Saito, H., Matsunaga, H., Okamoto, H., and Uozumi, Y. 2004. Preliminary stomach contents analysis of pelagic fishes collected by Shoyo-Maru 2002 research cruise in the Atlantic Ocean. Collect. Vol. Sci. Pap. ICCAT, **56**(3): 1096–1114.

Schaefer, K.M., and Fuller, D.W. 2002. Movements, behavior, and habitat selection of bigeye tuna (*Thunnus obesus*) in the eastern equatorial Pacific, ascertained through archival tags. Fish. Bull. **100**(4): 765–788.

Schaefer, K.M., and Fuller, D.W. 2005. Behavior of bigeye (*Thunnus obesus*) and skipjack (*Katsuwonus pelamis*) tunas within aggregations associated with floating objects in the equatorial eastern Pacific. Mar. Biol. **146**(4): 781–792. doi:10.1007/s00227-004-1480-x.

Schaefer, K.M., and Fuller, D.W. 2010. Vertical movements, behavior, and habitat of bigeye tuna (*Thunnus obesus*) in the equatorial eastern Pacific Ocean, ascertained from archival tag data. Mar. Biol. **157**(12): 2625–2642. doi:10.1007/s00227-010-1524-3.

Sibert, J., Lutcavage, M.E., Nielsen, A., Brill, R.W., and Wilson, S.G. 2006. Interannual variation in large-scale movement of Atlantic bluefin tuna (*Thunnus thynnus*) determined from pop-up satellite archival tags. Can. J. Fish. Aquat. Sci. **63**(10): 2154–2166. doi:10.1139/f06-114.

Sibert, J., Senina, I., Lehodey, P., and Hampton, J. 2012. Shifting from marine reserves to maritime zoning for conservation of Pacific bigeye tuna (*Thunnus obesus*). Proc. Natl. Acad. Sci. U.S.A. **109**(44): 18221–18225. doi:10.1073/pnas.1209468109. PMID:23064639.

Song, L.M., Xu, L.X., and Chen, X.J. 2005a. Preliminary analysis of the biological characteristics of bigeye tuna (*Thunnus obesus*) sampled from China tuna longlining fleet in central Atlantic Ocean. Collect. Vol. Sci. Pap. ICCAT, **58**(1): 292–296.

Song, L.M., Xu, L.X., and Chen, X.J. 2005b. Preliminary analysis of the relationship between bigeye tuna (*Thunnus obesus*) vertical distribution and the temperature, salinity in the central Atlantic Ocean. Collect. Vol. Sci. Pap. ICCAT, **58**(1): 297–303.

Song, L.M., Zhou, J., Zhou, Y., Nishida, T., Jiang, W., and Wang, J. 2009. Environmental preferences of bigeye tuna, *Thunnus obesus*, in the Indian Ocean: an application to a longline fishery. Environ. Biol. Fishes, **85**(2): 153–171. doi:10.1007/s10641-009-9474-7.

Staudinger, M.D., Juanes, F., Salmon, B., and Teffer, A.K. 2012. The distribution, diversity, and importance of cephalopods in top predator diets from offshore habitats of the Northwest Atlantic Ocean. Deep Sea Res. Part II Top. Stud. Oceanogr. **95**: 182–192. doi:10.1016/j.dsr2.2012.06.004.

Vaske, T., Travassos, P.E., Hazin, F.H.V., Tolotti, M.T., and Barbosa, T.M. 2012. Forage fauna in the diet of bigeye tuna (*Thunnus obesus*) in the western tropical Atlantic Ocean. Braz. J. Oceanogr. **60**(1): 89–97. doi:10.1590/S1679-87592012000100009.

Walli, A., Teo, S.L.H., Boustany, A., Farwell, C.J., Williams, T., Dewar, H., Prince, E., and Block, B.A. 2009. Seasonal movements, aggregations and diving behavior of Atlantic bluefin tuna (*Thunnus thynnus*) revealed with archival tags. PloS ONE, **4**(7): e6151. doi:10.1371/journal.pone.0006151. PMID:19582150.

Wilson, S.G., Lutcavage, M.E., Brill, R.W., Genovese, M.P., Cooper, A.B., and Everly, A.W. 2005. Movements of bluefin tuna (*Thunnus thynnus*) in the northwestern Atlantic Ocean recorded by pop-up satellite archival tags. Mar. Biol. **146**(2): 409–423. doi:10.1007/s00227-004-1445-0.

Wood, S.N. 2006. Generalized additive models: an introduction with R. Chapman & Hall.

Zavala-Camin, L.A. 1977. Distribución del patudo (*Thunnus obesus*) en el sudeste y sur del Brasil (1969-1977). Bol. Inst. Pesca, **5**(1): 40–50.

Zhu, G.P., Dai, X.J., Song, L.M., and Xu, L.X. 2011. Size at sexual maturity of bigeye tuna *Thunnus obesus* (Perciformes: Scombridae) in the tropical waters: a comparative analysis. Turk. J. Fish. Aquat. Sci. **11**(1): 145–152.

Zuyev, G., Nigmatullin, C., Chesalin, M., and Nesis, K. 2002. Main results of long-term worldwide studies on tropical nektonic oceanic squid genus *Sthenoteuthis*: an overview of the Soviet investigations. Bull. Mar. Sci. **71**(2): 1019–1060.

List of supplementary tables and figures

Figure S1. Model predictions on daily mean maximum depth of bigeye tuna.
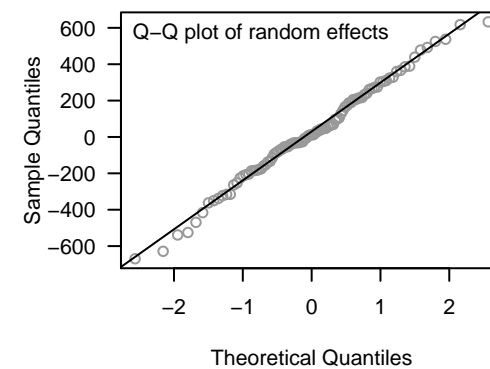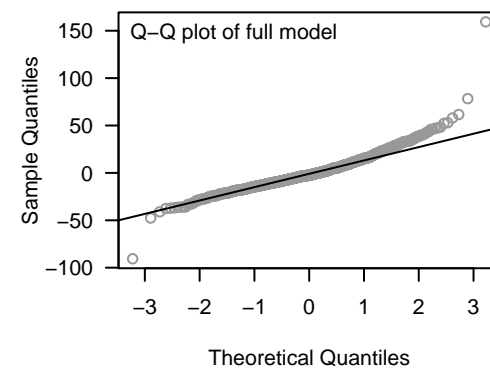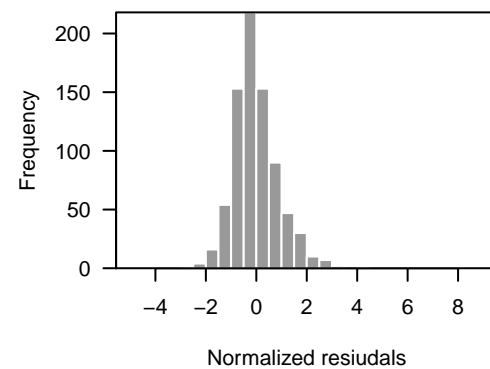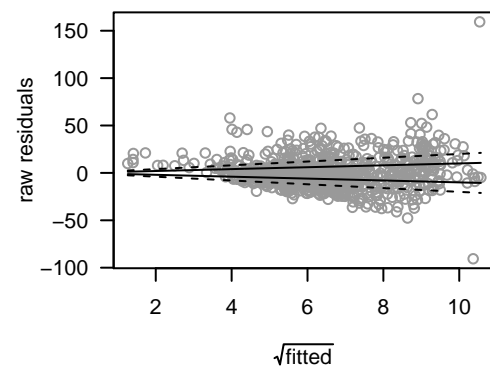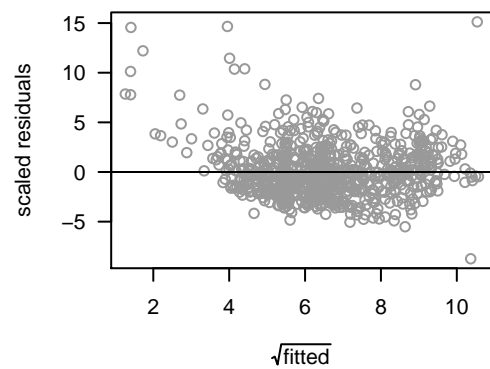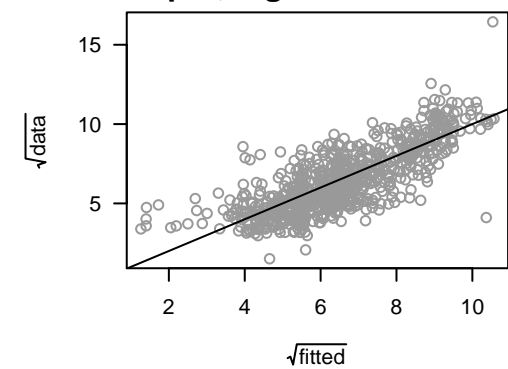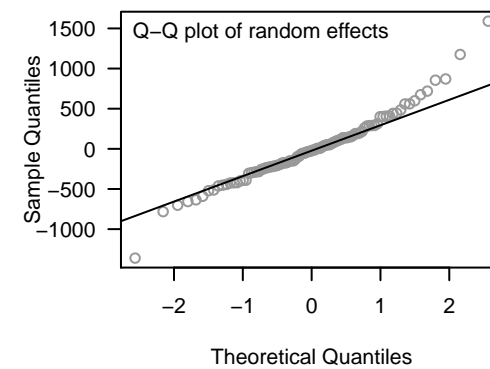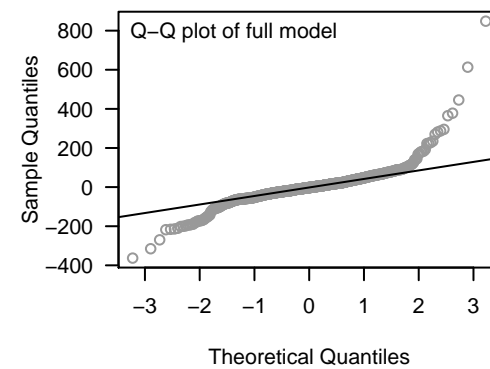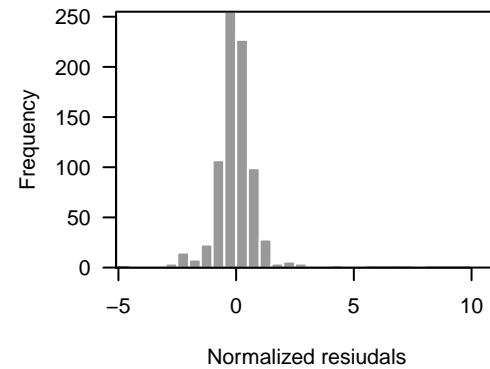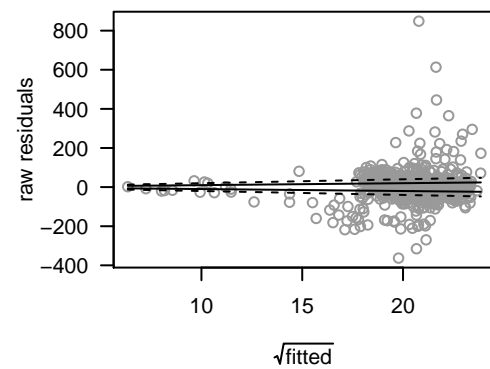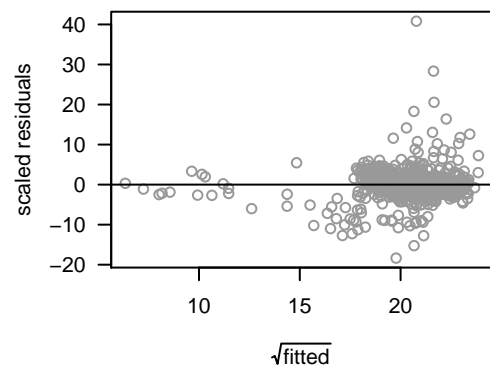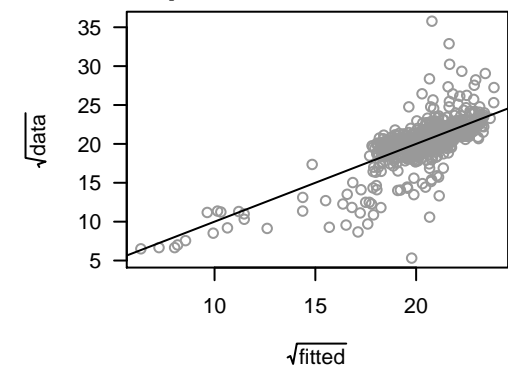
Figure S2. Diagnostic plots for GAMM models on daily vertical activity (daytime depth, nighttime depth, maximum depth, daytime temperature, nighttime temperature) of bigeye tuna. Six plots are available for each model (from left to right): 1) square-root-transformed fitted values versus square-root-transformed observed values, 2) Pearson residuals versus square-root-transformed fitted values, 3) raw residuals versus square-root-transformed fitted values, 4) distribution of normalized residuals, 5) quantile-quantile (Q-Q) plot for Pearson residuals of the full model, and 6) Q-Q plot for Pearson residuals of the random effect (tagged fish). To aid visualization, a 1:1 line for plots 1, 5 and 6, a zero-centered line for plot 2, and lines of 1 standard deviation (solid) and 2 standard deviation (dotted) for plot 3 are added.